Selection and identification of ligand peptides targeting a model of castrate-resistant osteogenic prostate cancer and their receptors

Jami Mandelin[a,1,2], Marina Cardó-Vila[b,c,1], Wouter H. P. Driessen[a,1,3], Paul Mathew[a,4], Nora M. Navone[a], Sue-Hwa Lin[a], Christopher J. Logothetis[a], Anna Cecilia Rietz[b,c], Andrey S. Dobroff[b,c], Bettina Proneth[a,5], Richard L. Sidman[d,6], Renata Pasqualini[b,c,6,7], and Wadih Arap[b,e,6,7]

[a]David H. Koch Center, Department of Genitourinary Medical Oncology, The University of Texas M. D. Anderson Cancer Center, Houston, TX 77030; [b]University of New Mexico Cancer Center and Divisions of [c]Molecular Medicine and [e]Hematology and Oncology, Department of Internal Medicine, University of New Mexico School of Medicine, Albuquerque, NM 87131; and [d]Harvard Medical School and Department of Neurology, Beth Israel Deaconess Medical Center, Boston, MA 02215

Contributed by Richard L. Sidman, January 19, 2015 (sent for review December 10, 2014)

We performed combinatorial peptide library screening in vivo on a novel human prostate cancer xenograft that is androgen-independent and induces a robust osteoblastic reaction in bone-like matrix and soft tissue. We found two peptides, PKRGFQD and SNTRVAP, which were enriched in the tumors, targeted the cell surface of androgen-independent prostate cancer cells in vitro, and homed to androgen receptor-null prostate cancer in vivo. Purification of tumor homogenates by affinity chromatography on these peptides and subsequent mass spectrometry revealed a receptor for the peptide PKRGFQD, α-2-macroglobulin, and for SNTRVAP, 78-kDa glucose-regulated protein (GRP78). These results indicate that GRP78 and α-2-macroglobulin are highly active in osteoblastic, androgen-independent prostate cancer in vivo. These previously unidentified ligand–receptor systems should be considered for targeted drug development against human metastatic androgen-independent prostate cancer.

peptides | ligand receptors | phage display | GRP78 | tumor targeting

Androgen deprivation remains the standard therapy for metastatic prostate cancer. Despite the favorable initial response, in most cases the disease progresses, becomes androgen-independent, and gives rise to soft tissue and osteoblastic bone metastases that ultimately lead to death (1, 2). Paradoxically, all currently available animal models of osteoblastic bone metastases are androgen dependent (3–6). The first (to our knowledge) human prostate cancer xenograft model that does not express androgen receptor but still induces a strong osteogenic response led Li et al. (7) to conclude that androgen receptor-null cells contribute to the castrate-resistant osteoblastic progression of prostate cancer and that targeting these cells will be critical in the treatment of prostate cancer bone metastases.

In vivo phage display can be used to explore the surface of cells in their anatomical microenvironment (8–14). This technology enables the identification of molecular signatures that could allow targeted systemic delivery of therapeutic agents to cancer tissues (9, 12, 15, 16). Using such methodology and the special prostate cancer model (7), we hypothesized that ligand–receptor pairs for targeting metastasizing androgen-independent prostate cancer cells could be identified.

Here we select two novel ligand peptides that were selected in vivo from human androgen-independent prostate cancer xenografts. We show that they target the surface of an androgen-independent prostatic cell line in vitro and home to androgen receptor-null prostate tumors in vivo. With affinity chromatography, we next isolated their respective receptors, 78-kDa glucose-regulated protein (GRP78) and α-2-macroglobulin, from tumor lysates and as a proof of principle verified the peptide–GRP78 interaction in vitro with recombinant GRP78. These data confirm that GRP78 is a functional molecular target on prostatic cancer cell surfaces in vivo. Such ligand–receptor systems may be applicable to targeted therapy and should be considered for validation against androgen-independent metastatic tumors.

Results

In Vivo Selection of Prostatic Tumor-Homing Peptides. We chose this novel prostate cancer xenograft model to select specific phage that home in vivo to bone-metastasizing tumors. The model is unique because it induces robust osteoblastic reaction despite its androgen independence (7). Mineralized tissue is formed during tumor growth when the tumor is implanted into s.c. pockets (Fig. 1*A*). Histological tumor specimens show dense bonelike tissue surrounded by soft prostate tumor tissue (Fig. 1*B*).

To determine whether the soft tissue and bonelike matrix compartments of the tumor differed from each other, we divided the tumor into two compartments during the selection. This division was achieved by manual microdissection of the bone from the tumor soft tissue after the phage had circulated for 24 h. The recovered phage pools were maintained separately thereafter. The enrichment of phage in both soft tissue and bonelike matrix

Significance

This study shows how phage display technology can be applied successfully to in vivo models and can advance molecular oncology through the identification of tumor-homing peptides and their target receptors. Treatment options are still limited for prostate cancer patients who have progressed to develop castrate-resistant osteoblastic bone metastases. The peptides identified in this study may lead to breakthroughs in fighting metastatic androgen-independent prostate cancer by enabling drug targeting and nanotechnology-based therapeutic strategies and may lead to significant advances in the management and therapy of this frequently lethal disease.

Author contributions: R.L.S., R.P., and W.A. designed research; J.M., M.C.-V., W.H.P.D., A.S.D., and B.P. performed research; J.M., M.C.-V., and W.H.P.D. analyzed data; and M.C.-V., P.M., N.M.N., S.-H.L., C.J.L., A.C.R., R.L.S., R.P., and W.A. wrote the paper.

The authors declare no conflict of interest.

Freely available online through the PNAS open access option.

[1]J.M., M.C.-V., and W.H.P.D. contributed equally to this work.

[2]Present address: Department of Medicine, University of Helsinki, FI-00014 Helsinki, Finland.

[3]Present address: Roche, Basel CH-4070, Switzerland.

[4]Present address: Department of Hematology/Oncology, Tufts Medical Center, Boston, MA 02111.

[5]Present address: Institute of Developmental Genetics, Helmholtz Zentrum München, 85764 Neuherberg, Germany.

[6]To whom correspondence may be addressed. Email: richard_sidman@hms.harvard.edu, rpasqual@salud.unm.edu, or warap@salud.unm.edu.

[7]R.P. and W.A. contributed equally to this work.

www.pnas.org/cgi/doi/10.1073/pnas.1500128112

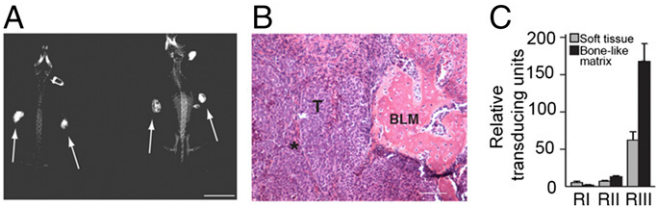

Fig. 1. Selection of tumor-homing phage in androgen-independent prostate cancer xenograft. (*A*) X-ray of mice 9 wk after s.c. implantation of human prostate cancer on the flanks. Note the mineralized tissue that is clearly visible in X-rays (arrows). (Scale bar, 2 cm.) (*B*) H&E staining of a section of a prostate cancer xenograft shows the bonelike matrix compartment (BLM) surrounded by tumor (T) and stromal cells (*). (Scale bar, 100 μm.) (*C*) Enrichment of phage in the prostate cancer xenograft. Phage were injected i.v. and allowed to circulate for 24 h. Soft tissue and bonelike matrix compartments were separated physically after the tumors were collected and were processed separately. The increase in relative transducing units in both tissue compartments indicates selective phage homing to the xenograft.

compartments is shown in Fig. 1*C*. The amount of phage recovered from the soft tissue compartment was enriched 12-fold after two rounds of enrichment. The enrichment of the phage in the bonelike matrix compartment was even more striking: After two rounds of selection, the enrichment increased 80-fold.

We sequenced 96 individual colonies of the plated bacterial culture aliquots from each round of selection. The recovered peptides displayed by the phage differed in the soft tissue and bonelike matrix compartments. The predominant sequences enriched in round 2 remained the same in round 3. After round 3, the three predominant phage clones recovered from the soft tissue compartment comprised 89% of the total peptide sequences. The corresponding value for two phage clones recovered from the bonelike matrix compartment was 48% (Table 1). Three predominant peptides (PKRGFQD, RIDAGTT, and SGPTRGM) that were displayed on the surface of the phage and recovered from soft tissue and one of peptides recovered from bonelike matrix (SNTRVAP) were amplified individually for further analysis.

Individual Phage Clones Home to Tumors upon Systemic Administration. To investigate the homing of the selected phage, we injected each clone i.v. into tumor-bearing mice. After 24 h, the mice were killed, and the tumors and several control organs were collected for analysis by phage staining. Substantial staining of the tumors for each phage clone was detected, whereas only background staining was observed in control organs. Negative-control phage was not detected in tumors or in several of the control organs. However, the location of the phage in the tumors differed among phage clones. PKRGFQD phage were localized predominantly in cancer cells, whereas SGPTRGM phage appeared in the stroma and capsule of the tumor. RIDAGTT phage also were observed in the tumor cells, but the immunoreactivity appeared to be weaker than that of PKRGFQD phage. As expected, the immunoreactivity of SNTRVAP phage was detected in the tumor cells near or within the bonelike matrix (Fig. 2).

PKRGFQD and SNTRVAP Phage Are Internalized by Prostatic Cancer Cells. Next, we evaluated whether tumor-homing peptides would be internalized by prostatic tumor cells in vitro. We used the bone metastasis-derived, androgen-independent PC-3 cell line as representative of human prostate cancer-derived cells. Osteosarcoma and Kaposi's sarcoma cells were used as controls. Each phage clone, insertless negative control, or RGD-4C–positive control phage (9, 16, 17) was incubated with cells. Consistent with the homing in vivo, internalization of PKRGFQD and SNTRVAP phage was detected in PC-3 cells, but internalization of SGPTRGM and RIDAGTT phage was not. Control cells did not internalize any of the prostate cancer-homing phage, whereas all cell types readily internalized the control RGD-4C phage. No internalization was detected with insertless phage (Fig. 3).

GRP78 Is the Receptor for SNTRVAP. To identify receptors recognizing the tumor-homing phage, we used immobilized PKRGFQD, RIDAGTT, SGPTRGM, or SNTRVAP synthetic peptides to purify their binding partners from tumor homogenates. Because the peptides could have shared receptor(s), an unrelated control peptide affinity column was used to control nonspecific binding of the proteins to the resin. Eluted proteins were resolved on polyacrylamide gels and subsequently were stained. Each column bound high-molecular-weight proteins that were not found in other columns (Fig. 4 *A* and *B*). Unique proteins were excised from the gel and analyzed by mass spectrometry. Proteins from other columns that displayed similar mobility on SDS/PAGE were also analyzed by mass spectrometry as controls. The analysis confirmed that different high-molecular-weight proteins were eluted from each column. Two of the peptides bound to serum proteins: PKRGFQD interacted with α-2-macroglobulin, and SGPTRGM interacted with ceruloplasmin. Fibulin-1 was recovered from the column coupled with RIDAGTT. The SNTRVAP column bound GRP78.

Given that GRP78 is associated with metastatic androgen-independent prostate cancer and enables tumor targeting by circulating ligands (15, 18, 19), we confirmed that proteins purified

Table 1. Peptides recovered from prostate cancer xenograft

Round 1		Round 2		Round 3	
Peptide	Frequency, %	Peptide	Frequency, %	Peptide	Frequency, %
Soft tissue compartment					
GGSQGAY	2.1	RIDAGTT	8.4	RIDAGTT	37.6
		PKRGFQD	4.2	SGPTRGM	33.3
		SPSQRQY	2.1	PKRGFQD	18.3
		GQVGIWS	2.1	PGDQPRG	3.2
		SGPTRGM	2.1	LDGPRAS	2.2
		GSQQQGR	2.1		
		PGDQPRG	1.1		
Bonelike matrix compartment					
None		SNTRVAP	11.7	SNTRVAP	33.7
		RLGLAWG	2.1	RLGLAWG	14.5
		VTRGVGF	2.1	SNNFVAP	3.6
				GAGPASV	2.4
				SNTFVAP	2.4

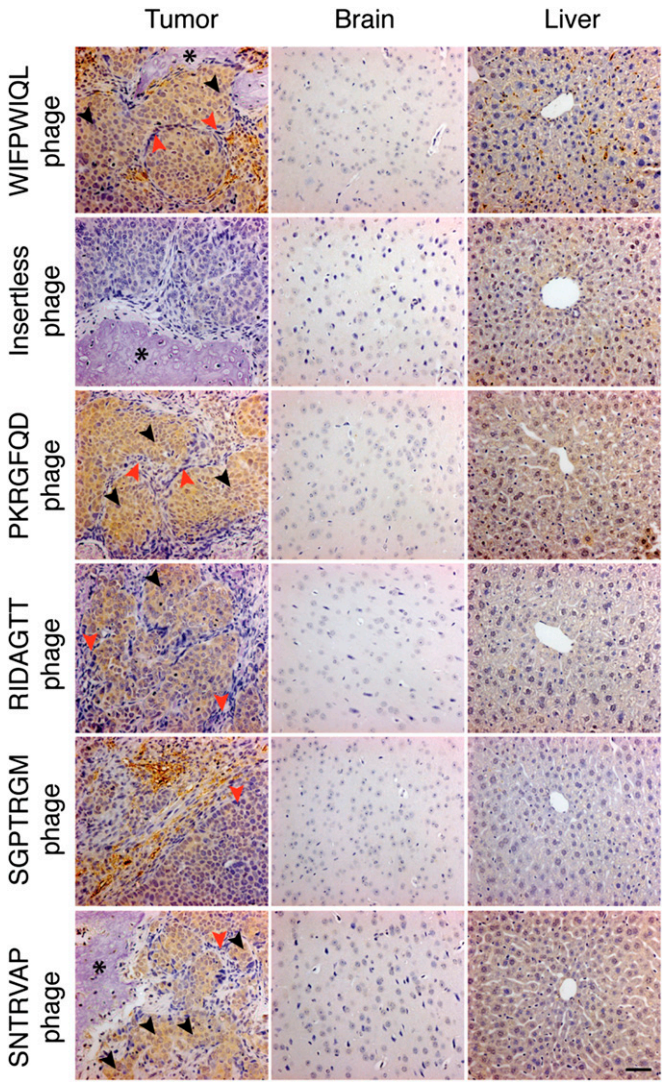

Fig. 2. Immunohistochemical staining of phage after i.v. injection into mice. Each individual phage clone, allowed to circulate for 24 h in tumor-bearing animals, homed specifically to the androgen-independent prostate cancer xenograft. Positive control phage with the WIFPWIQL insert, which binds to GRP78 and homes to prostate tumors (15), were detected in tumor cells and also in the stroma of the tumor. Phage containing the PKRGFQD insert were detected generally in tumor cells in all areas of the tumor, whereas phage containing the SGPTRGM insert were detected predominantly in stromal cells and in the tumor capsule. Phage with the RIDAGTT insert exhibited similar distribution similar to that of the PKRGFQD phage but a weaker immunoreactivity. Phage containing the SNTRVAP insert recovered from the bonelike matrix compartment of the tumor were found predominantly in tumor cells adjacent to bonelike tissue. Insertless phage were not detected in the tumor. Only background levels of immunoreactivity were detected in control organs (brain and liver). (Scale bar, 100 μm.)

by other peptides did not contain GRP78 (Fig. 4*B*). In addition, we validated the binding of SNTRVAP to GRP78. SNTRVAP phage and positive-control WIFPWIQL phage (15) bound to recombinant GRP78 in microtiter wells. The binding was specific, because there was no interaction with 70-kDa heat-shock cognate (Hsc70) or with BSA. Hsc70 protein was selected as a control because it belongs to the same heat-shock protein family as GRP78 and also was eluted from the SNTRVAP column. Insertless negative control phage did not bind to any of the proteins (Fig. 4*C*). We also observed a complete inhibition of SNTRVAP phage and WIFPWIQL phage binding to GRP78 by the corresponding synthetic peptides. Notably, WIFPWIQL peptide did not affect the binding of SNTRVAP phage, and SNTRVAP peptide did not affect the binding of WIFPWIQL phage (Fig. 4*D*).

Discussion

The treatment options for metastatic androgen-independent prostate cancer (20, 21) are limited. The lack of clinically relevant prostate cancer models has hampered the discovery of important molecules that permit androgen independence and therefore could be used as therapeutic targets. Recently, Li et al. (7) developed a novel prostate cancer xenograft model that did not express androgen receptor, grew in castrated SCID mice, and induced robust osteoblastic reactions. We used this model to perform in vivo phage display exploring functional receptors expressed on metastatic androgen-independent prostatic cancer cells. The aim was to discover new ligand–receptor pairs that could be used for targeted therapies.

Another advantage of this model is that it clearly induces the formation of bonelike tissue inside the tumor. Unlike tumors that grow inside bone, it is relatively easy to distinguish and separate its soft tissue and bone compartments in this model, so that the differentially homing phage can be identified. Sequences specifically enriched in each compartment did not appear in the other during the selection rounds, a result allowing two important conclusions: (*i*) selection and enrichment were highly specific, and (*ii*) the tumor microenvironment of the soft tissue compartment is different from that of tumors that reside inside or adjacent to bone.

To confirm the specific homing of the phage, we injected each individual clone into the circulation of tumor-bearing mice and visualized the clones in the tissues by immunostaining. According to the selection results, the phage that were enriched in the soft tissue compartment (PKRGFQD, RIDAGTT, and SGPTRGM) homed predominantly to soft tissue. The phage clone SNTRVAP, which was selected from the bonelike matrix compartment, homed to tumor cells within and adjacent to bonelike tissue. The location of different phage clones inside the soft tissue compartment varied significantly. PKRGFQD and RIDAGTT phage were observed in tumor cells, but SGPTRGM was seen only in the stroma and capsule of the tumor. Similar results were obtained with cultured tumor cells. PKRGFQD and SNTRVAP phage were internalized by an androgen-independent prostate cancer cell line but not by control sarcoma cell lines. SGPTRGM phage therefore appear to target the stromal cells of the tumor, and the receptor for this peptide is not abundant in tumor cells. In contrast, receptors for PKRGFQD and SNTRVAP phage are present on the surface of prostatic cancer cells but not on the surface of other cell types used here.

We were able to identify putative binding partners for all phage clones by affinity purification with synthetic peptides. Fibulin-1 was purified with RIDAGTT peptide. Fibulin-1 is present in the stroma of several ovarian cancers and cysts (22) and in normal bone marrow stroma (23). It also makes breast cancer cells more resistant to doxorubicin (24). Interestingly, *fibulin-1* expression is decreased in prostate cancer compared with normal prostate epithelium but is accumulated inside prostate cancer cells despite the low expression levels (25). Therefore it is feasible that prostate cancer cells in vitro do not produce fibulin-1 and do not internalize RIDAGTT phage. However, prostate cancer cells in vitro might take up fibulin-1–bound RIDAGTT phage from the stroma.

By SGPTRGM peptide-affinity chromatography, we purified ceruloplasmin, a copper-binding protein in plasma that is angiogenic at high concentrations (26). The level of ceruloplasmin is increased in certain cancers (27–29) such as prostate cancer (30, 31) and after estrogen administration (32, 33). Copper-chelating agents (e.g., tetrathiomolybdate) lower ceruloplasmin levels and are potent antiangiogenic agents, but their clinical efficacy in the treatment of metastatic androgen-independent prostate cancer still awaits

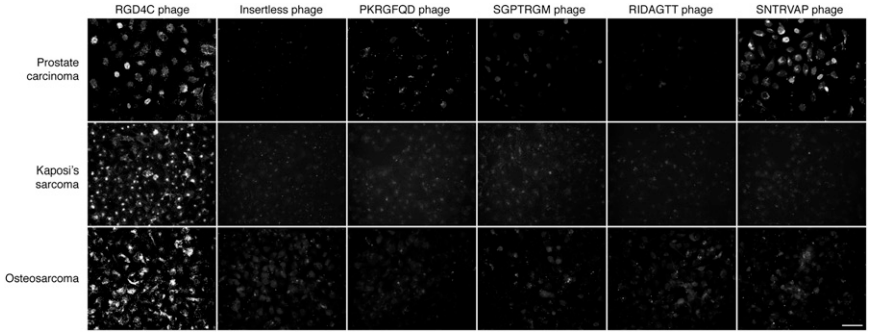

Fig. 3. Phage internalization by human prostate carcinoma PC-3, Kaposi's sarcoma, or osteosarcoma cell lines. PKRGFQD, SGPTRGM, RIDAGTT, SNTRVAP, RGD-4C (positive control), or insertless (negative control) phage were incubated with human cancer-derived cell lines for 12 h at 37 °C to allow phage internalization. PKRGFQD and SNTRVAP phage were internalized by prostate carcinoma cells but not by sarcoma cells. SGPTRGM and RIDAGTT were not internalized by any cell type. RGD-4C phage were internalized by all cell types, and insertless phage were not internalized by any cell type that was tested. (Scale bar, 30 μm.)

verification (34). It is most likely that SGPTRGM phage was bound to ceruloplasmin in plasma and was transported to the tumor with ceruloplasmin.

PKRGFQD peptide bound specifically to α-2-macroglobulin in tumor homogenates. α-2-Macroglobulin is a plasma protein that interacts with and entraps virtually any protease and thereby affects access to the respective substrates. It also interacts with several cytokines and hormones and modulates their activity (35). In patients with prostate cancer, α-2-macroglobulin is proteolytically activated and signals predominantly through GRP78 to promote the proliferation and survival of cancer cells (36, 37). The levels of both native and activated α-2-macroglobulin in serum decrease during disease progression (38). Our observations suggest that prostatic cancer cells readily take up α-2-macroglobulin from serum, because the phage with the insert PKRGFQD most likely binds to the α-2-macroglobulin present in the circulation before internalization of the whole complex by the cells.

GRP78 protein was purified with SNTRVAP peptide. This protein is a stress-inducible, multifunctional, prosurvival, endoplasmic reticulum chaperone that belongs to the HSP70 family. GRP78 is composed of an ATPase domain, a peptide binding-domain, and a C-terminal domain of unknown function (39–44). Several different cell types, including proliferating endothelial cells as well as tumor cells, express GRP78 on their surface (15, 45–55). Notably, expression of GRP78 correlates with the development of metastatic androgen-independent disease and with poor survival (19, 56–59). Our results confirm these previous findings and emphasize the presence of GRP78 in the bone metastases from prostate cancer.

In summary, we discovered peptides that target metastatic androgen-independent prostate cancer in a relevant new human xenograft model. Affinity purification identified proteins that are all associated with cancer progression. In particular, α-2-macroglobulin and GRP78 are clearly implicated in the development of metastatic prostate cancer (35, 38, 48, 56, 58, 59). We previously targeted prostate cancer with phage that bind to GRP78 (15). However, in contrast to these previously described phage, those described here were selected from a naive library in vivo, and their homing capacities appear to be superior to those of the earlier constructs (15). Thus the ligand peptides that we have identified in this report seem to be promising candidates for targeting metastatic androgen-independent prostate cancer.

Materials and Methods

Reagents. CB17 SCID mice were purchased from Charles River Laboratories. The fUSE5-based phage peptide library displaying cyclic random peptides (CX_7C, in which C represents cysteine, and X represents a random amino acid) has been described previously (12, 56). Cellgro cell and bacterial culture media were purchased from Mediatech. FBS, vitamins, nonessential amino acids, antibiotics, glutamine, and trypsin were from Gibco. Cell culture and plastic disposables were from BD Biosciences; Lab-Tek II Chamber Slides for internalization assays were from Nalge Nunc International. Individual protease inhibitors were from Sigma. Complete protease inhibitor mixture was from Roche. Rabbit anti-fd bacteriophage IgG was from Sigma, Cy3-conjugated goat anti-rabbit IgG was from Jackson ImmunoResearch Laboratories, and the EnVision+ System for immunohistochemistry was from DAKO. Peptides were synthesized as cyclic peptides to our specifications by PolyPeptide Laboratories. The unrelated peptide CARAC was used as a negative control unless otherwise specified. The CarboxyLink peptide immobilization kit was from Pierce. Millex filter units and Microcon YM-10 centrifugal filter units were purchased from Millipore. The Quick Start Bradford Protein Assay and all protein electrophoresis reagents were from Bio-Rad. SimplyBlue SafeStain Coomassie staining reagent was from Invitrogen. Endoproteinase trypsin (modified, sequencing grade) was obtained from Promega. All other chemicals used in proteolytic digestion and HPLC were obtained from Sigma. The Quadrupole ion trap mass spectrometer used in the proteomic analysis was manufactured by Thermo. The nonredundant protein database was downloaded from the National Center for Biotechnology Information GenBank database. Recombinant GRP78 and Hsc70 were from Stressgen Bioreagents. Rabbit anti-GRP78 IgG was from Sigma. Common laboratory chemicals were purchased from Fisher Scientific or Sigma.

Prostate Cancer Xenograft. Collection and phenotypic characterization of the MDA PCa 118b prostate cancer bone metastasis specimen has been described (7). Briefly, the specimen was obtained by needle biopsy from the sacroiliac zone of an exophytic osteoblastic lesion in the left hemipelvis of a 49-y-old Caucasian male with androgen-independent prostate cancer. The specimen was placed immediately in cold (4 °C) sterile α-MEM (alpha Eagle's minimum essential medium), and small pieces subsequently were implanted into s.c. pockets of 6- to 8-wk-old male CB17 SCID mice. Mice were monitored weekly for tumor growth. All animal experimentation was reviewed and approved by the Institutional Animal Care and Use Committee at the University of Texas M. D. Anderson Cancer Center.

In Vivo Screening of Prostate Cancer Xenograft with the Phage Library. In vivo selection of tumor homing-peptides was performed as described (56), with the following modifications. For round 1, tumor-bearing mice received 2×10^9 transducing units (TU) of phage peptide library i.v. After 24 h of circulation, the mice were perfused with 10 mM PBS (pH 7.4), and tumors were collected. Soft tissue and bonelike matrix compartments of the tumor were separated physically, weighed, and homogenized for phage recovery. The recovered phage pool was amplified and subjected to another round of selection. Recovered pools from soft tissue and bonelike matrix compartments were administered separately into different tumor-bearing mice. Three rounds of selection were performed.

Phage Recovery. Soft tissues of the tumor were homogenized with a glass Dounce homogenizer, and bonelike matrix tissues of the tumor were homogenized with a mortar and pestle under liquid nitrogen. Tissue homogenates were suspended in 1 mL of DMEM containing proteinase inhibitors (DMEM-prin; 1 mM phenylmethylsulphonyl fluoride, 20 μg/mL aprotinin, and

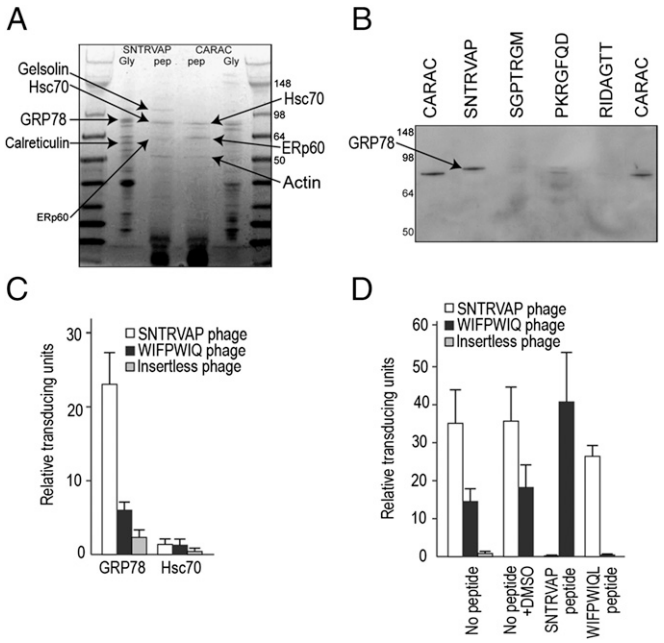

Fig. 4. GRP78 is a receptor for SNTRVAP phage. (*A*) Typical electrophoresis of proteins after affinity purification. Four micrograms of protein from peptide columns after peptide (pep) and glycine (Gly) elution were resolved on 4–20% SDS-polyacrylamide gels and were visualized with SimplyBlue SafeStain reagent. Unique proteins were excised and sent for mass spectrometric analysis. Control column purifications were performed simultaneously from exactly the same protein lysates, and proteins of similar size also were subjected to mass spectrometry. (*B*) A representative Western blot of proteins after affinity purification. Protein (0.25 μg) from peptide columns after glycine elution were resolved on 10% SDS-polyacrylamide gels, blotted, and visualized with anti-GRP78 antibody. SNTRVAP peptide from affinity columns bound GRP78 protein not found in other columns. (*C*) Phage containing the SNTRVAP insert bound specifically to GRP78. GRP78, Hsc70, or BSA was coated on microtiter wells at 1 μg/mL, and the wells were incubated with SNTRVAP, and with WIFPWIQL phage as positive controls (15) or with an insertless phage as a negative control. Results are expressed as mean ± SEM of triplicate wells, relative to BSA. (*D*) Phage binding was blocked by a synthetic peptide. Because WIFPWIQL was solubilized in DMSO, phage binding also was performed in the presence of DMSO. SNTRVAP specifically blocked the binding of SNTRVAP phage, but not that of WIFPWIQL phage, to recombinant GRP78. Similarly, WIFPWIQL specifically blocked binding of WIFPWIQL phage but not that of SNTRVAP phage. An insertless phage served as a negative control. Results are expressed as mean ± SEM of triplicate wells, relative to BSA.

1 μg/mL leupeptin), vortexed, and washed three times with DMEM-prin. The homogenates next were incubated with 1 mL of host bacteria (log-phase *Escherichia coli* K91kan; OD_{600} ~2). Aliquots of the bacterial culture were plated onto LB agar plates containing 40 μg/mL tetracycline and 100 μg/mL kanamycin. Plates were incubated overnight at 37 °C.

Phage Homing Assay. Tumor-bearing mice under general anesthesia (Tribromoethanol; 250 mg/kg) received 2×10^{10} TU i.v. of PKRGFQD, RIDAGTT, SGPTRGM, SNTRVAP, or insertless phage. Phage were allowed to circulate for 24 h. The mice subsequently were perfused, and the organs were collected. Half of each organ was snap-frozen in liquid nitrogen, and the other half was fixed in 10% (vol/vol) buffered formalin (pH 7.4). Tumors from left and right sides were frozen and fixed after soft tissue and bonelike tumor matrix compartments were separated. For phage staining, the bonelike matrix compartments were decalcified in PBS containing 10% (vol/vol) EDTA. All tissues were embedded in paraffin and were sectioned for staining. Frozen tissues were processed as described in the previous section. After infection, serial dilutions of the infections were plated, and the number of infective particles on these plates was counted on the next day.

Phage Staining. The sections were rehydrated and deparaffinized. After peroxidase- and protein-blocking steps, the phage were detected with rabbit anti-fd bacteriophage antibody (1:1,000 dilution). HRP-conjugated secondary antibody followed by 3,3′-diaminobenzidine-tetrahydrochloride chromogen was used to visualize the phage. Sections were counterstained with hematoxylin, dehydrated, and mounted. All washes before chromogen were performed with 0.05% Tween-20 (Sigma-Aldrich) in 50 mM Tris-buffered saline (pH 7.4).

Phage Internalization Assay. PC-3 prostate carcinoma, KRIB osteosarcoma, and Kaposi's sarcoma cells (5×10^4) were incubated with 5×10^9 TU of PKRGFQD, RIDAGTT, SGPTRGM, SNTRVAP, RGD-4C (positive control phage; refs. 9, 16, 17), or insertless fd-tet phage (negative control) in chamber slides for 12 h. After extensive washes, the cells were fixed, rendered permeable, and blocked with 1% BSA in PBS. The internalized phage was detected with rabbit anti-fd bacteriophage antibody (diluted 1:100) and Cy3-conjugated anti-rabbit antibody (1:200).

Receptor Purification. PKRGFQD, RIDAGTT, SGPTRGM, SNTRVAP, and unrelated control peptide columns were prepared with 5 mg of each peptide per the manufacturer's instructions. Tumors were collected from perfused animals; soft tissue and bonelike matrix compartments were separated physically and weighed, and 1.5 g of the bone compartment was homogenized under liquid nitrogen. Proteins were extracted in PBS containing 1 mM $CaCl_2$, 1 mM $MgCl_2$, 50 mM n-octyl-β-D-glucopyranoside, 1% Triton X-100, 0.2 mM PMSF, and complete protease inhibitor (Roche Life Science). After 1-h incubation at 4 °C, the extract was cleared by centrifugation at $12,000 \times g$ for 30 min. The cleared extract was filtered through a 0.45-μm PVDF syringe filter unit, and the protein concentration was measured. Twelve milligrams of protein extract was applied to SNTRVAP and unrelated control peptide columns. After extensive washing with PBS containing 0.01 mM $CaCl_2$, 0.01 mM $MgCl_2$, 50 mM n-octyl-β-D-glucopyranoside, 0.2 mM phenylmethylsulphonyl fluoride, and Complete protease inhibitors, the bound proteins were eluted in 1-mL fractions with 4 mM target peptide in washing buffer. All bound proteins were recovered in 1-mL fractions from a further elution with 0.1 M glycine in 0.1 M NaCl (pH 3.0) and were monitored by absorbance at 280 nm. Peak fractions were pooled and concentrated for protein determination. Four micrograms of protein were resolved on 4–20% SDS-polyacrylamide gels, and bands were visualized with SimplyBlue SafeStain reagent. Protein bands of interest were excised and analyzed by mass spectrometry.

Western Blotting. The protein samples of glycine fractions (0.25 μg) were resolved on 10% SDS-polyacrylamide gels and were blotted onto nitrocellulose membranes; GRP78 was visualized with anti-GRP78 antibody (1: 1,000).

Proteomic Analysis. Proteins were identified at ProtTech, Inc. in conjunction with nanoLC-MS/MS peptide-sequencing technology. Each gel band was destained, cleaned, and digested in-gel with sequencing-grade trypsin. The resulting peptide mixture was analyzed by an LC-MS/MS system, in which HPLC with a 75-μm i.d. reverse-phase C18 column was coupled in line with an ion-trap mass spectrometer. The acquired mass spectrometric data served to search the most recent nonredundant protein database with ProtTech's proprietary software suite. The output from the database search was validated manually before reporting.

Phage Binding to GRP78. Phage-binding assays on recombinant GRP78, Hsc70, and BSA were conducted as described (15, 57). Briefly, proteins were immobilized on microtiter wells (1 μg per well) overnight at 4 °C. Wells were washed twice with PBS, blocked with 3% (wt/vol) BSA in PBS for 2 h at room temperature, and incubated with 10^9 TU of SNTRVAP and WIFPWIQ phage clones or insertless fd-tet phage in 50 μL PBS containing 2% (wt/vol) BSA. After 1 h at room temperature, the wells were washed 10 times with PBS, and bound phage were recovered by bacterial infection. Synthetic SNTRVAP and WIFPWIQ peptides (10 μM) were used to evaluate the specificity of phage binding to GRP78. All experiments were done in duplicate and were repeated at least four times with similar results.

ACKNOWLEDGMENTS. We thank Dr. Helene Sage for insightful discussions and Dr. Fernanda Staquicini, Connie Sun, and Jun Yang for technical assistance. This work was supported by National Cancer Institute Specialized Program of Research Excellence in Prostate Cancer, the Prostate Cancer Foundation, the Gillson-Longenbaugh Foundation (R.P. and W.A.), Helsingin Sanomat Centennial Foundation, the Emil Aaltonen Foundation, the Research and Science Foundation of Farmos, the Maud Kuistila Memorial Foundation, the Instrumentarium Science Foundation (J.M.), and the Susan G. Komen Breast Cancer Foundation (M.C.-V.).

1. Hadaschik BA, Sowery RD, Gleave ME (2007) Novel targets and approaches in advanced prostate cancer. *Curr Opin Urol* 17(3):182–187.
2. Logothetis CJ, Lin SH (2005) Osteoblasts in prostate cancer metastasis to bone. *Nat Rev Cancer* 5(1):21–28.
3. Corey E, et al. (2002) Establishment and characterization of osseous prostate cancer models: Intra-tibial injection of human prostate cancer cells. *Prostate* 52(1):20–33.
4. Lee YP, et al. (2002) Use of zoledronate to treat osteoblastic versus osteolytic lesions in a severe-combined-immunodeficient mouse model. *Cancer Res* 62(19):5564–5570.
5. Thalmann GN, et al. (2000) LNCaP progression model of human prostate cancer: Androgen-independence and osseous metastasis. *Prostate* 44(2):91–103.
6. Yang J, et al. (2001) Prostate cancer cells induce osteoblast differentiation through a Cbfa1-dependent pathway. *Cancer Res* 61(14):5652–5659.
7. Li ZG, et al. (2008) Androgen receptor-negative human prostate cancer cells induce osteogenesis in mice through FGF9-mediated mechanisms. *J Clin Invest* 118(8): 2697–2710.
8. Pasqualini R, Ruoslahti E (1996) Organ targeting in vivo using phage display peptide libraries. *Nature* 380(6572):364–366.
9. Arap W, Pasqualini R, Ruoslahti E (1998) Cancer treatment by targeted drug delivery to tumor vasculature in a mouse model. *Science* 279(5349):377–380.
10. Ellerby HM, et al. (1999) Anti-cancer activity of targeted pro-apoptotic peptides. *Nat Med* 5(9):1032–1038.
11. Arap W, et al. (2002) Steps toward mapping the human vasculature by phage display. *Nat Med* 8(2):121–127.
12. Arap W, et al. (2002) Targeting the prostate for destruction through a vascular address. *Proc Natl Acad Sci USA* 99(3):1527–1531.
13. Kolonin MG, et al. (2006) Synchronous selection of homing peptides for multiple tissues by in vivo phage display. *FASEB J* 20(7):979–981.
14. Yao VJ, et al. (2005) Targeting pancreatic islets with phage display assisted by laser pressure catapult microdissection. *Am J Pathol* 166(2):625–636.
15. Arap MA, et al. (2004) Cell surface expression of the stress response chaperone GRP78 enables tumor targeting by circulating ligands. *Cancer Cell* 6(3):275–284.
16. Hajitou A, et al. (2006) A hybrid vector for ligand-directed tumor targeting and molecular imaging. *Cell* 125(2):385–398.
17. Pasqualini R, Koivunen E, Ruoslahti E (1997) Alpha v integrins as receptors for tumor targeting by circulating ligands. *Nat Biotechnol* 15(6):542–546.
18. Kim Y, et al. (2006) Targeting heat shock proteins on cancer cells: Selection, characterization, and cell-penetrating properties of a peptidic GRP78 ligand. *Biochemistry* 45(31):9434–9444.
19. Mintz PJ, et al. (2003) Fingerprinting the circulating repertoire of antibodies from cancer patients. *Nat Biotechnol* 21(1):57–63.
20. Scher HI, et al. (2005) Cancer of the prostate. *Cancer Principles and Practise of Oncology*, eds DeVita VT, Jr, Hellman S, Rosenberg SA (Lippincott Williams & Wilkins, Philadelphia), 7th Ed.
21. Lauer RC, Friend SC, Rietz C, Pasqualini R, Arap W (2015) Drug design strategies for the treatment of prostate cancer. *Expert Opin Drug Discov* 10(1):81–90.
22. Clinton GM, et al. (1996) Estrogens increase the expression of fibulin-1, an extracellular matrix protein secreted by human ovarian cancer cells. *Proc Natl Acad Sci USA* 93(1):316–320.
23. Gu YC, Nilsson K, Eng H, Ekblom M (2000) Association of extracellular matrix proteins fibulin-1 and fibulin-2 with fibronectin in bone marrow stroma. *Br J Haematol* 109(2): 305–313.
24. Pupa SM, et al. (2007) Regulation of breast cancer response to chemotherapy by fibulin-1. *Cancer Res* 67(9):4271–4277.
25. Wlazlinski A, et al. (2007) Downregulation of several fibulin genes in prostate cancer. *Prostate* 67(16):1770–1780.
26. Ziche M, Jones J, Gullino PM (1982) Role of prostaglandin E1 and copper in angiogenesis. *J Natl Cancer Inst* 69(2):475–482.
27. Green JA, Pocklington T, Dawson AA, Foster M (1980) Electron spin resonance studies on caeruloplasmin and iron transferrin in patients with chronic lymphocytic leukaemia. *Br J Cancer* 41(3):356–359.
28. Lamoureux G, Mandeville R, Poisson R, Legault-Poisson S, Jolicoeur R (1982) Biologic markers and breast cancer: A multiparametric study—1. Increased serum protein levels. *Cancer* 49(3):502–512.
29. Shifrine M, Fisher GL (1976) Ceruloplasmin levels in sera from human patients with osteosarcoma. *Cancer* 38(1):244–248.
30. Fotiou K, et al. (2007) Serum ceruloplasmin as a marker in prostate cancer. *Minerva Urol Nefrol* 59(4):407–411.
31. Nayak SB, Bhat VR, Upadhyay D, Udupa SL (2003) Copper and ceruloplasmin status in serum of prostate and colon cancer patients. *Indian J Physiol Pharmacol* 47(1): 108–110.
32. Briggs MH (1978-1979) Biochemical basis for the selection of oral contraceptives. *Int J Gynaecol Obstet* 16(6):509–517.
33. Doe RP, Mellinger GT, Swaim WR, Seal US (1967) Estrogen dosage effects on serum proteins: A longitudinal study. *J Clin Endocrinol* 27:1081–1086.
34. Henry NL, et al. (2006) Phase II trial of copper depletion with tetrathiomolybdate as an antiangiogenesis strategy in patients with hormone-refractory prostate cancer. *Oncology* 71(3-4):168–175.
35. Borth W (1992) Alpha 2-macroglobulin, a multifunctional binding protein with targeting characteristics. *FASEB J* 6(15):3345–3353.
36. Misra UK, Deedwania R, Pizzo SV (2006) Activation and cross-talk between Akt, NF-kappaB, and unfolded protein response signaling in 1-LN prostate cancer cells consequent to ligation of cell surface-associated GRP78. *J Biol Chem* 281(19): 13694–13707.
37. Misra UK, Pizzo SV (2012) Receptor-recognized α_2-macroglobulin binds to cell surface-associated GRP78 and activates mTORC1 and mTORC2 signaling in prostate cancer cells. *PLoS ONE* 7(12):e51735.
38. Sinnreich O, et al. (2004) Plasma levels of transforming growth factor-1beta and alpha2-macroglobulin before and after radical prostatectomy: Association to clinicopathological parameters. *Prostate* 61(3):201–208.
39. Jolly C, Morimoto RI (2000) Role of the heat shock response and molecular chaperones in oncogenesis and cell death. *J Natl Cancer Inst* 92(19):1564–1572.
40. King LS, et al. (2001) Isolation, expression, and characterization of fully functional nontoxic BiP/GRP78 mutants. *Protein Expr Purif* 22(1):148–158.
41. Lee AS (2007) GRP78 induction in cancer: Therapeutic and prognostic implications. *Cancer Res* 67(8):3496–3499.
42. Luo S, Baumeister P, Yang S, Abcouwer SF, Lee AS (2003) Induction of Grp78/BiP by translational block: Activation of the Grp78 promoter by ATF4 through and upstream ATF/CRE site independent of the endoplasmic reticulum stress elements. *J Biol Chem* 278(39):37375–37385.
43. Luo S, Mao C, Lee B, Lee AS (2006) GRP78/BiP is required for cell proliferation and protecting the inner cell mass from apoptosis during early mouse embryonic development. *Mol Cell Biol* 26(15):5688–5697.
44. Wooden SK, Lee AS (1992) Comparison of the genomic organizations of the rat grp78 and hsc73 gene and their evolutionary implications. *DNA Seq* 3(1):41–48.
45. Davidson DJ, et al. (2005) Kringle 5 of human plasminogen induces apoptosis of endothelial and tumor cells through surface-expressed glucose-regulated protein 78. *Cancer Res* 65(11):4663–4672.
46. Delpino A, Piselli P, Vismara D, Vendetti S, Colizzi V (1998) Cell surface localization of the 78 kD glucose regulated protein (GRP 78) induced by thapsigargin. *Mol Membr Biol* 15(1):21–26.
47. Gonzalez-Gronow M, et al. (2006) Prostate cancer cell proliferation in vitro is modulated by antibodies against glucose-regulated protein 78 isolated from patient serum. *Cancer Res* 66(23):11424–11431.
48. Shani G, et al. (2008) GRP78 and Cripto form a complex at the cell surface and collaborate to inhibit transforming growth factor beta signaling and enhance cell growth. *Mol Cell Biol* 28(2):666–677.
49. Takemoto H, et al. (1992) Heavy chain binding protein (BiP/GRP78) and endoplasmin are exported from the endoplasmic reticulum in rat exocrine pancreatic cells, similar to protein disulfide-isomerase. *Arch Biochem Biophys* 296(1):129–136.
50. Triantafilou M, Fradelizi D, Triantafilou K (2001) Major histocompatibility class one molecule associates with glucose regulated protein (GRP) 78 on the cell surface. *Hum Immunol* 62(8):764–770.
51. Xiao G, Chung TF, Pyun HY, Fine RE, Johnson RJ (1999) KDEL proteins are found on the surface of NG108-15 cells. *Brain Res Mol Brain Res* 72(2):121–128.
52. Sokolowska I, Woods AG, Gawinowicz MA, Roy U, Darie CC (2012) Identification of a potential tumor differentiation factor receptor candidate in prostate cancer cells. *FEBS J* 279(14):2579–2594.
53. Liu R, et al. (2013) Monoclonal antibody against cell surface **GRP78** as a novel agent in suppressing PI3K/AKT signaling, tumor growth, and metastasis. *Clin Cancer Res* 19(24):6802–6811.
54. Lee AS (2014) Glucose-regulated proteins in cancer: Molecular mechanisms and therapeutic potential. *Nat Rev Cancer* 14(4):263–276.
55. Rasche L, et al. (2013) The natural human IgM antibody PAT-SM6 induces apoptosis in primary human multiple myeloma cells by targeting heat shock protein GRP78. *PLoS ONE* 8(5):e63414.
56. Rauschert N, et al. (2008) A new tumor-specific variant of **GRP78** as target for antibody-based therapy. *Lab Invest* 88(4):375–386.
57. Daneshmand S, et al. (2007) Glucose-regulated protein GRP78 is up-regulated in prostate cancer and correlates with recurrence and survival. *Hum Pathol* 38(10): 1547–1552.
58. Pootrakul L, et al. (2006) Expression of stress response protein Grp78 is associated with the development of castration-resistant prostate cancer. *Clin Cancer Res* 12(20 Pt 1): 5987–5993.
59. Roller C, Maddalo D (2013) The molecular chaperone GRP78/BiP in the development of chemoresistance: Mechanism and possible treatment. *Front Pharmacol* 4:10.